

A. NOWOTNIK*, L. BŁAŻ**, T. SIWECKI***, J. SIENIAWSKI*

PHASE TRANSFORMATION DURING HOT DEFORMATION OF 0.16%C STEEL

PRZEMIANA FAZOWA STALI 0,16% W WARUNKACH ODKSZTAŁCANIA WYSOKOTEMPERATUROWEGO

Effect of hot deformation process and transformation Austenite(A)→ Ferrite(F) and Austenite→Pearlite(P) on a carbon steel (0.158%C) microstructure was studied. Hot compression test at constant strain rate were performed during controlled cooling of the sample within the temperature range related to the start and finish of these phase transformations. Attention was paid to structural effects of dynamic precipitation and resulted morphology of structural components dependent on expected localization of phase transformation. It was shown that the flow localization during hot deformation and preferred growth of the pearlite colonies at shear bands was very limited. The most characteristic feature of the microstructure observed for hot deformed samples was the development of carbides that nucleated along elongated ferrite grains.

Keywords: carbon steel, phase transformation, dynamic precipitation, hot deformation, CCT diagram

W pracy przedstawiono wyniki badań wpływu odkształcania wysokotemperaturowego i przemiany Austenit(A)→ Ferryt(F) oraz Austenit→Perlit(P) na mikrostrukturę stali węglowej (0.158%C). Przeprowadzono próby ściskania w warunkach kontrolowanego chłodzenia ze stałą prędkością odkształcania. Odkształcenia realizowano w czasie przejścia przez temperaturowy zakres przemiany fazowej. Uwagę szczególną zwrócono na obserwację mikrostruktury i morfologię składników fazowych mogących potwierdzić proces niejednorodnego wydzielania związanego z lokalizacją przemiany. Wykazano, że w warunkach dynamicznych nieciągła przemiana stali praktycznie nie charakteryzuje się skłonnością do lokalizacji spowodowanej niejednorodnością odkształcenia. Najistotniejszą cechą mikrostruktury stali po odkształceniu w zakresie przemiany jest wydzielanie węglików na granicach odkształconych ziarn ferrytu.

1. Introduction

During hot deformation of solution treated alloy at the temperature below a *solvus temperature* a dynamic precipitation is expected. It was reported that an interaction of deformation process and discontinuous transformation in Cu-Ti and CuNiCrSiMg alloys result in very strong flow localization that promote discontinuous phase transformation at shear bands and following dynamic coagulation of precipitates [2, 3, 4]. It was concluded that discontinuous precipitation intensifies non-uniform deformation process. Within the shear bands there are a number of microstructural events, which may occur during hot deformation. In a course of strain localization, fragmentation of the precipitates and their effective coagulation was responsible for the local decrease of the flow resistance. As a result, the flow stress decrease was observed. Since the discon-

tinuous precipitation leads to similar microstructure of mentioned alloys and hypo-eutectoid carbon steel, one may expect that also austenite (A) to ferrite (F) and austenite to pearlite (P) transformation in particular in steel can result in localized flow under hot deformation conditions.

From structural point of view, eutectoidal transformation in carbon steel may leads to creation of similar structure containing discontinuous reaction product – colonies of pearlite – localized along shear bands as had been observed for CuTi and AlNiSiCrMg alloys [2-4]. One may presume therefore that the effect of the localized distribution of structural components can also develop in carbon steel hot deformed within the range of *discontinuous transformation* of Austenite→Pearlite. The analysis of dynamic structural processes in carbon and alloyed steel [5, 6] is focused on discussion of experiments carried out in the range of austenite or stable

* RZESZÓW UNIVERSITY OF TECHNOLOGY, WINCENTEGO POLA 2, RZESZÓW, POLAND

** UNIVERSITY OF SCIENCE AND TECHNOLOGY, MICKIEWICZA 30, KRAKÓW, POLAND

*** CORROSION METALS RESEARCH INSTITUTE, DROTTNING KRISTINAS VÄG 48, STOCKHOLM, SWEDEN

structure created in result of foregoing eutectoidal reaction. There is a lack of data, which are referred to specific features of the dynamic processes (*dynamic recrystallization, dynamic precipitation*) that can occur during *discontinuous transformation* of A→P [6]. Therefore, the presented work provides “supplementary” information on structural aspects of the hot deformation process that develops during A→F and A→P transformation. In order to intensify an interaction of phase transformation and deformation processes, hot compression tests were performed at constant cooling rate within the temperature range corresponding to start and finish of A→F+P transformation.

2. Material and experimental procedure

Investigation were carried out on commercial carbon steel containing of 0.156%C, 0.21%Si, 0.62%Mn, 0.014%P, 0.012S and 0.005%Al (%mas.). Cylindrical specimens of 5 mm in diameter and 10mm in height were machined from cold drawn bar of 30 mm diameter. The specimens were heat treated at 1473 K for 30 min and then quenched into ice water. Phase transformation start and finish temperatures were detected due to dilatometer tests performed by means of Bähr DIL805A/D dilatometer testing equipment. The specimen was austenitized at 1473 K for 3 min and cooled down to room temperature with constant cooling rate of 0.2 – 300 K/s. Continuous cooling transformation (CCT) diagrams were constructed on the basis of received dilatation curves and metallographic examination of the specimens.

The second set of cylindrical specimens was used for compression experiments. Hot compression tests were performed on a Bähr DIL805A/D dilatometer equipped with special deformation unit. The specimens were prior-heated to 1473 K at a heating rate of 3 K/s, annealed for 3 min and cooled with constant cooling rate of 0.5, 1, 3, 5 and 10 K/s until A→P transformation finish temperature was reached. In order to execute fixed cooling rate of the sample, an automatically controlled argon or helium inflation was applied. Compression tests were performed at the strain rate of $0.004s^{-1}$ within the range of austenite to ferrite and pearlite transformation.

As soon as the test finished, the sample was cooled down to room temperature with forced helium gas. In order to avoid decarburization of the specimen surface, the experiments were performed in a vacuum chamber equipped with an induction heating system. High purity argon gas was used after evacuation of the chamber to 10^{-4} mbar to protect the sample oxidation. Load and sample length were recorded by a computer during deformation, and converted to stress-true strain curves after testing. Flat samples for structural observations were cut

from the specimens along longitudinal axis. The sample surface was prepared using standard grinding and polishing procedure and etched in 2 vol% Nital solution. Structure observations and hardness measurements were performed within a middle area of the specimen. A load of 4.905 N was used at the Vickers hardness test. Specimens for transmission electron microscopy were punched as 3 mm diameter discs then grounded to 50-100 μm and thinned by means PIPS 690-type ion thinning machine. Thin foils were examined by means of JEOL – JEM 2010 ARP transmission electron microscope at 200 kV.

3. Results

In order to choose accurate conditions for following compression test, a continuous cooling transformation diagrams were determined. CCT diagram of the examined steel was constructed using dilatometer tests at constant cooling rate. Complementary microstructure observation and hardness measurement results were used to confirm phase transformation effect (Fig. 1). As the following investigations are related to sole austenite to ferrite and pearlite transformation, an examination of the bainite formation area was neglected.

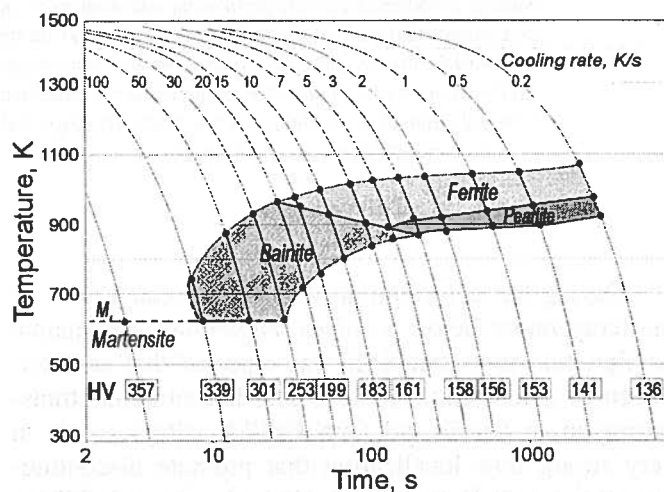


Fig. 1. CCT diagram for tested carbon steel. Sample cooling rate and related Vickers hardness of the material was marked in the figure

True stress – true strain curves received for tested steel at constant temperature of 873 K and 1023 K are shown in Fig. 2. The temperatures correspond to the start and finish temperature for A→F and A→P transformation. Third $\sigma_t - \epsilon_t$ curve was received during hot compression at constant strain rate and cooling of the sample within the temperature range of 1023 – 873 K. During deformation of the steel and continuous cooling within A→F+P transformation temperature range, an effective increase of the flow stress was observed.

Overlapping of deformation process and phase transformation intensified by cooling of the sample results in higher hardening of the material than that for the sample deformed at constant temperature of 873 K.

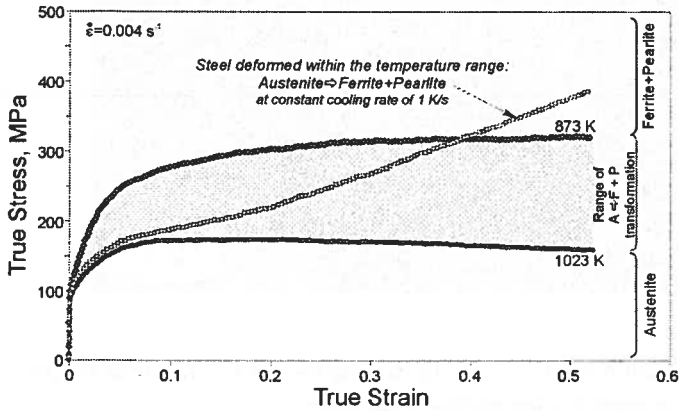


Fig. 2. True stress- true strain curves received for isothermally deformed samples at transformation start and finish temperatures, i.e. 1023 and 873 K respectively. Third $\sigma_t - \varepsilon_t$ curve was received during continuous cooling within the temperature range of 1023 K – 873 K

However, in spite of intense strain hardening due to deformation and phase transformation overlapping, microstructural observation of deformed sample did not reveal any flow localization effects or heterogeneous distribution of the microstructural components.

Complementary hot compression experiments were carried out on samples cooled with constant cooling rate ranging from 1 to 5 K/s and deformed within start and finish transformation temperature range. As a constant strain rate was used, samples were deformed with varied

true strain from 0.15 to 0.5 depending on the “passage time” through the phase transformation region (Fig. 3a).

True stress/true strain curves for samples deformed at different cooling rates are shown in Fig. 3b. Hardening rate as well the final flow stress value was found to increase with increasing cooling rate in spite of reduced deformation of the sample. As the strain rate was the same for each experiment, one can conclude that the hardening rate depends mostly on refining of structure components due to phase transformation being accelerated with increasing cooling rate. In particular, an effective hardening effect at largest cooling rate of 5 K/s can be ascribed to the ferrite grain refinement as well as early stage of bainite development at the end of compression test (Fig. 4b).

Microstructure of the sample deformed at true strain rate of 0.004s⁻¹ and cooling rate of 1 and 5 K/s are shown in Fig. 4a and Fig. 5 respectively. Typical microstructure observed in the central part of the sample revealed elongated ferrite grains as well as nearly uniform distribution of pearlite (Fig. 4a). However, in spite of some strain localization effect a meaningful localization of structural components along shear bands was not observed (see: regions marked with arrows in the figure).

Columnar colonies of pearlite were observed at outer part of the same sample cross section as marked schematically in Fig. 5 (upper-right corner). Similar effect of eutectoid reaction location was not observed in residual part of the sample section. Observed pearlite bands probably result from local carbon enrichment due to carbon segregation produced at casting procedure. Local carbon inhomogenities resulted in the development of elongated pearlite colonies after subsequent drawing

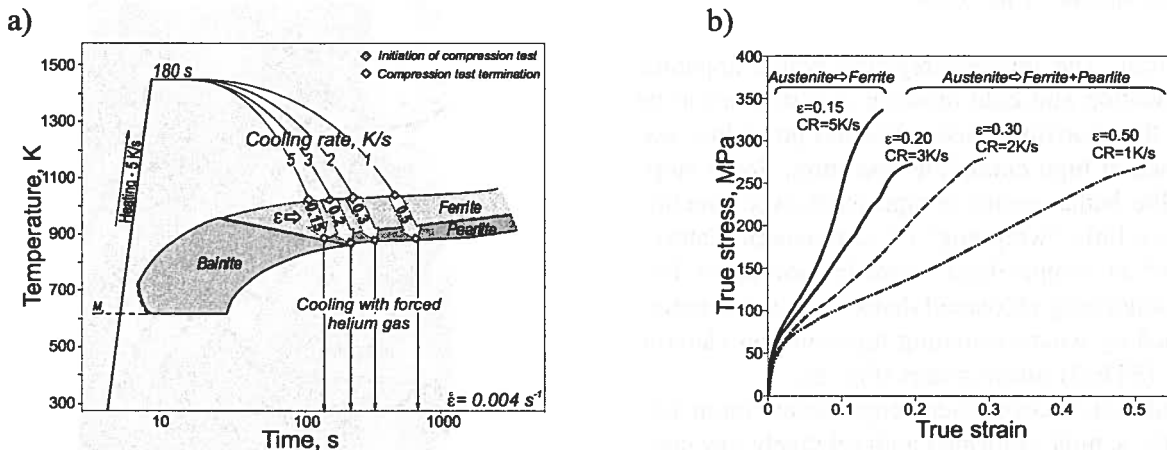


Fig. 3. CCT diagram and scheme of laboratory processing schedules; b) true stress- true strain curves received for samples deformed at strain rate of 0.004s⁻¹ and constant cooling rate. Final deformation of the sample, marked in the figure, was dependent on the time of passing through the transformation temperature range marked on CTT diagram

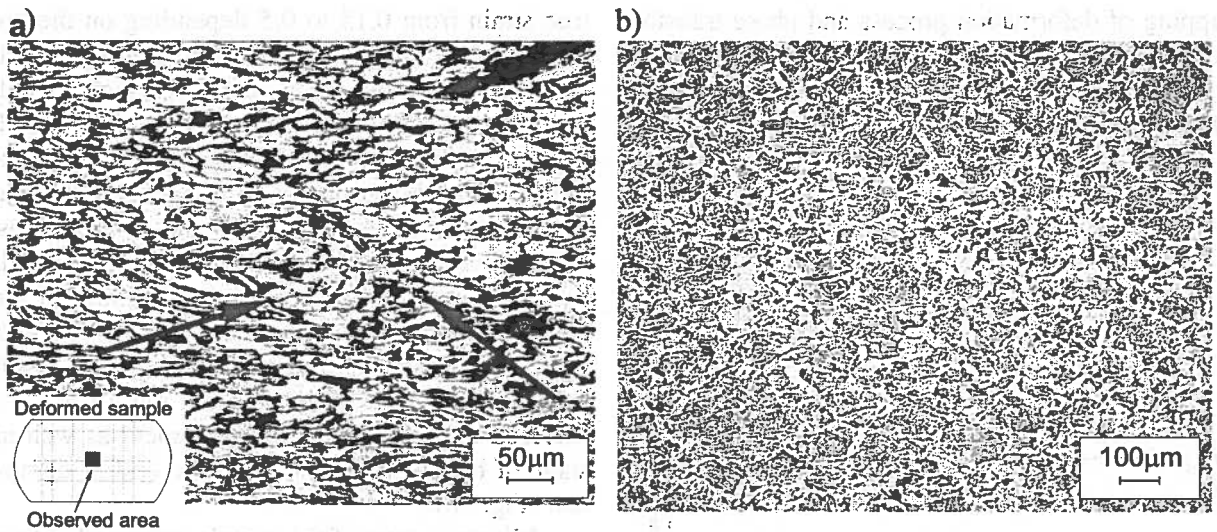


Fig. 4. Microstructure of the sample deformed during phase transformation A→F+P: a) $\epsilon_t = 0.5$, cooling rate CR = 1 K/s; b) $\epsilon_t = 0.15$, cooling rate CR = 5 K/s. Observed areas were marked schematically in the images

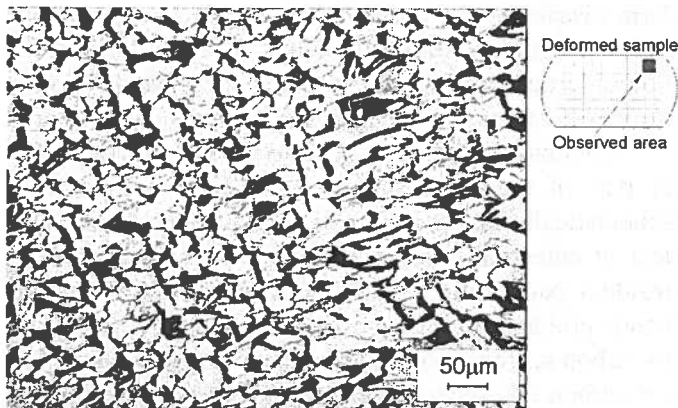


Fig. 5. Microstructure of the sample deformed $\epsilon_t = 0.5$ during phase transformation A→F+P at cooling rate CR = 1 K/s. Observed area was marked schematically in the picture

of the material. The microsegregation which appeared after solidification and cold drawing was difficult to be removed as the short-time austenitization procedure was not performed at high enough temperature. Some slope of the pearlite bands versus compression axis direction results from a little “wrapping” of compressed material at the edge of the sample due to some friction effect. Ferrite grains containing recovered dislocation substructure were revealed by means scanning transmission electron microscopy (STEM) observations (Fig. 6).

Transmission electron microscopy observations performed for the sample deformed with relatively low cooling rate (1K/s) and low strain rate did not practically reveal any shear bands development that would provide preferential sites for nucleation of pearlite or ferrite grains. Microstructural components have shown a random distribution in the material structure.

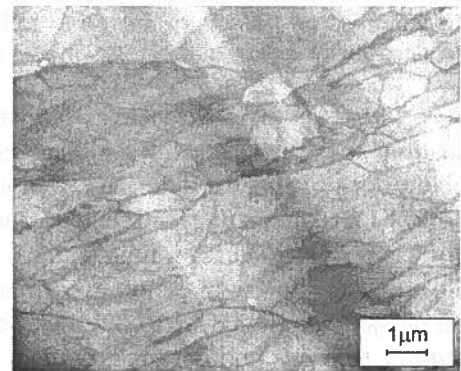


Fig. 6. STEM micrograph of the sample deformed $\epsilon_t = 0.5$ at cooling rate of 1 K/s within transformation temperature range



Fig. 7. TEM microstructure of the steel deformed with $\epsilon_t = 0.3$ during phase transformation at cooling rate of 2 K/s and strain rate of 0.004 s^{-1}

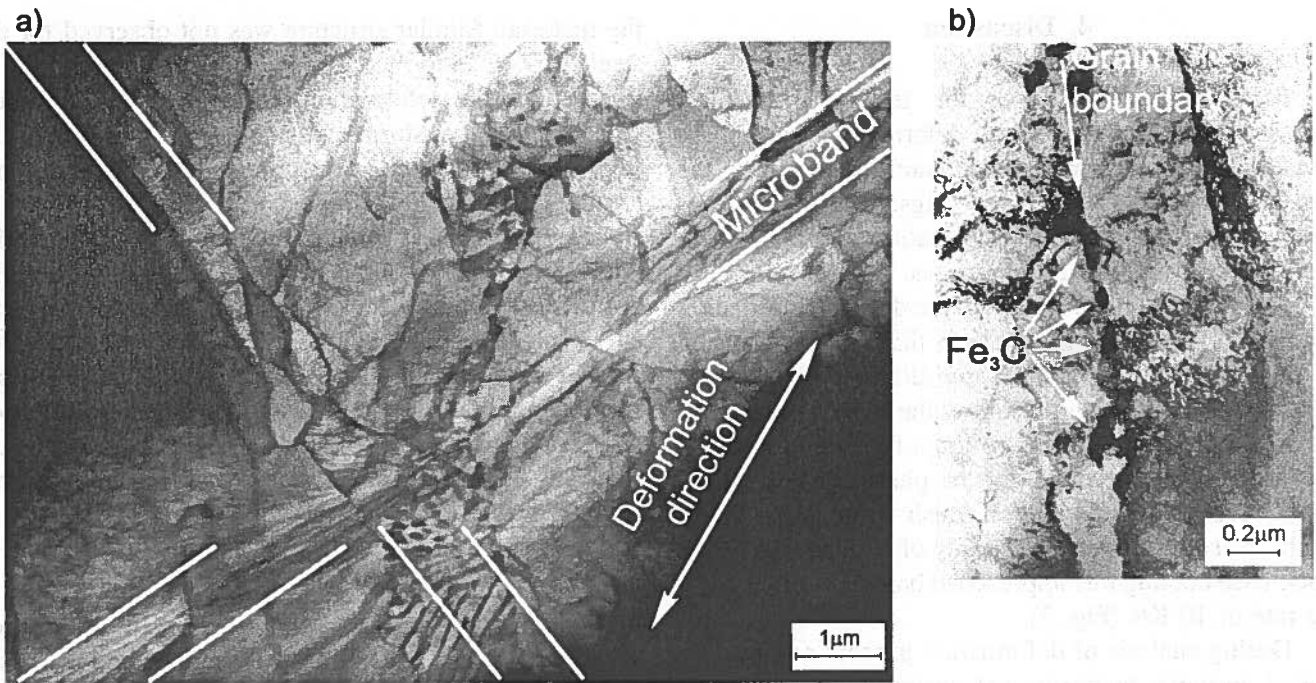


Fig. 8. Sample deformed during eutectoid transformation at cooling rate of 2 K/s ($\epsilon_t = 0.3$; strain rate 0.004 s^{-1}): a) pearlite colony presumably distributed along shear band; b) cementite particles distributed at elongated ferrite grain boundaries

It was concluded that relatively slow cooling rate and low strain rates did not practically cause any localization of $A \rightarrow F+P$ phase transformation. For this reason one more attempt was made to intensify microstructural processes with the increasing cooling rate. TEM observations confirmed practically a uniform distribution of structural components at the sample deformed at high cooling rate. Any noticeable shear bands development and related preferential nucleation of pearlite or ferrite grains was found. Commonly known pearlite colonies growth at ferrite grain boundaries was observed (Fig. 7).

TEM observations evidenced very few effects of non-uniform distribution of microstructural components that might result from preliminary flow localization (Fig. 8a). Elongated pearlite colonies development can be related to the flow localization and accelerated phase transformation along shearing area. Pearlite colonies shown in the figure were probably formed at two intersecting micro shear bands. This is however, rarely observed effect of structural heterogeneity that might be related to localized plastic flow and discontinuous transformation of $A \rightarrow F+P$. It worth to stress that the most distinguishable feature of the sample structure is related to preferred Fe_3C particles distribution along elongated ferrite boundaries (Fig. 8b).

Localized Fe_3C particles development at ferrite grain boundaries was often observed for other samples deformed at higher strain rates and higher cooling rate

(Fig. 9). TEM observations lead to a conclusion that the effect described above is the most essential feature of the localized form of nucleation during phase transformation and simultaneous deformation of the sample.

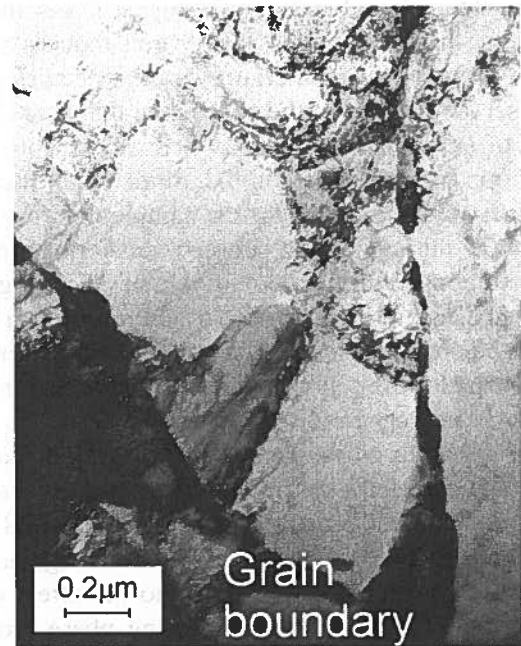


Fig. 9. Carbides at ferrite grain boundary. Sample deformed during phase transformation $A \rightarrow F+P$ ($\epsilon_t = 0.15$, strain rate: 0.004 s^{-1} , cooling rate: 5 K/s)

4. Discussion

Experimental conditions for testing mechanical and structural effects of hot deformation and phase transformation overlapping were carefully stated on the basis of received CCT curves (Figs. 1 and 3). It was assumed that the phase transformation can be slightly accelerated by deformation process. As a result, a real transformation finish temperature during deformation testing might become higher than that for static testing of CCT curves. In spite of some discrepancy of fixed transformation finish temperature, the temperature range for hot compression during cooling of the sample indeed covered temperature range for the phase transformation. An increase of transformation finish temperature might be the reason for special intensity of sample hardening while used cooling rate approached bainite range at cooling rate of 10 K/s (Fig. 2).

During analysis of deformation process and accompanied austenite to ferrite and austenite to pearlite reaction in carbon steel the main attention was paid for structural effects of strain/precipitation interaction and presumed microstructure inhomogeneities. An intense flow localization accompanied by discontinuous phase transformation within shear bands was reported for CuTi and CuNiCrSiMg alloys [2-4]. As received structure for both carbon steel and mentioned Cu-alloys looks similar, some localized effects of discontinuous precipitation along shear bands may also be expected in tested steel. As a result, an arrangement of ferrite grains and pearlite colonies along shear bands would appear if assume that a ferrite grain growth within shear bands induces a local recrystallization of the material. However, detailed structure observations lead to the conclusion that some localization of structural components with relation to strain localization bands was negligible. Some strain localization effects were observed for the sample deformed to a strain of 0.5 during cooling between transformation start and finish temperature at cooling rate of 1K/s (Fig. 4a). Localized distribution of pearlite might result from shear banding before phase transformation finish (area marked by arrows). However, similar structural inhomogeneities were observed very rarely.

It is worth to emphasize that well organized cementite plates elongated along common direction were observed within colonies of pearlite for eutectoidal steel cross-rolled at 1123 K and [6, 7]. An arrangement of structural components was ascribed to the effect of localized flow of austenite and following phase transformation during cooling of hot deformed steel. Resulted spatial organization of ferrite and cementite plates was concluded to result in "quasi-composite" structure of

the material. Similar structure was not observed for the steel 0.16%C deformed during phase transformation. It is probable that deformation conditions used for simultaneous phase transformation and hot deformation of the steel were not sufficient enough for shear banding and localized phase transformation.

Development of cementite precipitates along ferrite grain boundaries was the most noticeable effect of the hot deformation and subsequent transformation for tested samples (Figs 8b and 9). The effect was intensified with an increase of phase transformation intensity being enhanced by simultaneous cooling and deformation process. Similar feature of the sample structure was revealed by TEM for samples deformed high and moderate cooling rates.

5. Conclusions

1. Hot compression tests were performed at constant cooling rate in order to test mechanical and structural effects of simultaneous austenite to ferrite and pearlite transformation and deformation process for 0.156% steel. In spite of the fact that volume fraction of pearlite was relatively high, microstructural observations of hot deformed samples lead to a conclusion that localization of discontinuous phase transformation A→P is negligible compared to similar effects reported in a literature for CuTi and CuNiCrSiMg alloys.
2. Noticeable structural feature of the sample hot deformed during phase transformation was related to preferential growth of cementite particles at some boundaries of elongated and deformed ferrite grains.

REFERENCES

- [1] J.W. Christian, The theory of transformations in metals and alloys, Pergamon Press, Oxford Anglia, 1965.
- [2] M. Niewczas, E. Evangelista, L. Błaż, Scripta Metall. 27, 1735-1740 (1992).
- [3] A.A. Hamed, L. Błaż, Materials Science and Engineering, A254, 83-89 (1998).
- [4] A.A. Hamed, L. Błaż, Scripta Materialia 12, 1987-1993 (1997).
- [5] J.J. Jonas, I. Weiss, Met. Science 13, 238-245 (1979).
- [6] A. Korbel, W. Bochniak, F. Ciura, H. Dybiec, K. Pieła, Proceedings: Sessions and Symposia sponsored by the Extraction and Processing Division, held at the TMS Annual Meeting in Ontario, Florida USA, 301-312 (1997).
- [7] A. Korbel, W. Bochniak, F. Ciura, H. Dybiec, K. Pieła, Materials Processing Technology 78, 104-111 (1998).